Axonal Transport of the Mitochondria-specific Lipid, Diphosphatidylglycerol, in the Rat Visual System

WILLIAM D. BLAKER, JEFFRY F. GOODRUM, and PIERRE MORELL

Biological Sciences Research Center and Department of Biochemistry and Nutrition, University of North Carolina, Chapel Hill, North Carolina 27514. Dr. Blaker's present address is Lab Preclinical Pharmacology, National Institute of Mental Health, St. Elizabeth's Hospital, Washington, D.C. 20032.

ABSTRACT Rats 24 d old were injected intraocularly with [2-^{3}H]glycerol and [^{35}S]methionine and killed 1 h–60 d later. ^{35}S label in protein and ^{3}H label in total phospholipid and a mitochondria-specific lipid, diphosphatidylglycerol(DPG), were determined in optic pathway structures (retinas, optic nerves, optic tracts, lateral geniculate bodies, and superior colliculi). Incorporation of label into retinal protein and phospholipid was nearly maximal 1 h postinjection, after which the label appeared in successive optic pathway structures. Based on the time difference between the arrival of label in the optic tract and superior colliculus, it was calculated that protein and phospholipid were transported at a rate of about 400 mm/d, and DPG at about half this rate. Transported labeled phospholipid and DPG, which initially comprised 3–5% of the lipid label, continued to accumulate in the visual structures for 6–8 d postinjection.

The distribution of transported material among the optic pathway structures as a function of time differed markedly for different labeled macromolecules. Rapidly transported proteins distributed preferentially to the nerve endings (superior colliculus and lateral geniculate). Total phospholipid quickly established a pattern of comparable labeling of axon (optic nerve and tract) and nerve endings. In contrast, the distribution of transported labeled DPG gradually shifted toward the nerve ending and stabilized by 2–4 d. A model is proposed in which apparent "transport" of mitochondria is actually the result of random bidirectional saltatory movements of individual mitochondria which equilibrate them among cell body, axon, and nerve ending pools.

Although it is generally thought that nerve-ending mitochondria originate in the cell perikaryon, the rate at which they are transported between the two regions has been assigned a wide range of values. Optical analyses of the movements of individual elongated structures (presumably mitochondria) in axons generally have shown occasional saltatory motions which are equally distributed in the anterograde and retrograde directions (1–6). Results from labeling with amino acids or ^{59}Fe have been interpreted as indicating either intermediate (~50 mm/d) or slow (<10 mm/d) mitochondrial transport, although a small proportion of nerve-ending mitochondria were labeled rapidly (7–13). Measurements of accumulation of mitochondria (14) or mitochondrial enzymes (15–17) at nerve ligations have been interpreted as indicating their slow bidirectional transport.

We report here the transport kinetics and distribution of mitochondria as measured by labeled diphosphatidylglycerol (DPG), a lipid known to be synthesized only in mitochondria (18, 19). These results are compared to the transport behavior of other membrane lipids and proteins and interpreted in light of the special properties of mitochondria. In addition, the distribution of other transported macromolecules is presented and discussed.

MATERIALS AND METHODS

23- to 26-d-old Long-Evans rats, bred from animals obtained from Charles River Laboratories (Wilmington, Mass.), were placed under ether anesthesia and a mixture of 130–200 μCi of [2-^{3}H]glycerol (5–10 Ci/mmol), and 25–50 μCi of [^{35}S]methionine (600 Ci/mmol) in 5 μl of isotonic saline was injected into the vitreous humor of the left eye using a Hamilton 10-μl syringe (Hamilton Co., Reno, Nev.) with a replaceable 26-gauge needle. In some long-term experiments, 60 μCi of [^{32}P]orthophosphoric acid (carrier-free) replaced the [^{35}S]methionine. All radiolabeled compounds were obtained from New England Nuclear, Boston, Mass. In control experiments, animals were injected intraocularly with 1 μg of

colchicine (Sigma Chemical Co., St. Louis, Mo.) 24 h before and then again at the time of the injection of [^{3}H]glycerol.

Animals were killed 1 h–60 d later, and the retinas, optic nerves, and optic tracts (each about 10 mm in length), lateral geniculate bodies, and superior colliculi were dissected. Tissues were placed in 0.5 ml of water, optic nerves were longitudinally split to open the surrounding sheath and facilitate lipid extraction, lateral geniculate bodies and superior colliculi were homogenized, and all tissue samples were lyophilized and stored at −70°C. Lipids were extracted from accumulated samples by the addition of 0.1 ml of water followed by 2 ml of chloroform:methanol (2:1). 25 μg of carrier DPG was added to each lipid extract, and DPG was isolated by the one-dimensional thin-layer chromatographic method of Skipski and Barclay (20) for the separation of acidic phospholipids. In this system, neutral lipids are moved to the top of the plate with acetone-petroleum ether, 1:3 (vol/vol), and a second development with chloroform: methanol:acetic acid:water 80:13:8:0.3 (vol/vol) was used to move DPG to just beneath the neutral lipid band, with other phospholipids moving shorter distances as a function of their polarity. The appropriate band was scraped into a scintillation vial and, after the addition of 0.4 ml of water and 10 ml of Triton-X 100-based scintillation mixture (21), its radioactivity was determined by liquid scintillation counting. The entire lane below the DPG band was also scraped and its radioactivity was determined. This value was added to that of the DPG, and the sum was referred to as total phospholipid radioactivity. Less than 2% of the total lipid ^{32}P or ^{3}H was found to run above the DPG. The DPG obtained by the one-dimensional chromatographic separation was >90% radiochemically pure as determined by subsequent two-dimensional thin-layer chromatography (22).

For determination of [^{35}S]methionine-labeled macromolecules in each tissue, the upper phase plus insoluble material obtained during the two-phase lipid extraction was blown to dryness under nitrogen. 1 ml of water was added to the residue, followed by 1.0 ml of 20% trichloroacetic acid and 1% phosphotungstic acid 30 min later. After centrifugation, the supernate was removed and the insoluble material was dissolved overnight in 1 ml of Protosol (New England Nuclear). 10 ml of 0.3% 2,5-diphenyloxazole in xylene was added before liquid scintillation counting.

Transported radioactivity in each of the left optic nerves, right optic tracts, lateral geniculate bodies, and superior colliculi was corrected for systemic labeling by subtracting the radioactivity in the corresponding contralateral structure. This correction overestimates actual systemic labeling in the tracts, geniculates, and colliculi because of the presence of 5–10% uncorssed fibers in the rat visual system. The resultant values for 1–60 d were corrected for injection variability by normalizing to the mean of the retinal radioactivity levels at each time point. For the short time-course studies, values were normalized to the mean of the 1–8-h levels combined, because retinal labeling varied little during this period.

In one experiment, superior colliculi were fractionated 6 d after intraocular injection of [^{32}P]orthophosphoric acid. Tissues (60 mg wet wt) were homogenized in 9 vol of 0.32 M sucrose, 0.1 mM EDTA, pH 7.0. A crude nuclear fraction was prepared at 2,000 rpm for 5 min in 1-ml tubes fitting adaptors for the Sorvall SS34 rotor (DuPont Instruments-Sorvall, DuPont Co., Newtown, Conn.). The supernate was collected and the pellets were washed once under the same conditions. A crude mitochondrial fraction was prepared from the pooled supernate by centrifugation at 7,500 rpm for 15 min in the same rotor. This pellet was homogenized in 2 ml of 1.0 mM phosphate buffer, pH 8.3, and left on ice for 30 min. This lysed material was layered over a 10, 14, and 18% sodium diatrozoate gradient (23) and fractionated at 24,000 rpm for 15 min in a Spinco SW50 rotor (Beckman Instruments, Inc., Spinco Div., Palo Alto, Calif.). The mitochondrial pellet was collected, washed with 0.32 M sucrose, and recentrifuged at 7,500 rpm for 20 min in the Sorval SS34 rotor. Lipid analysis was as described above.

The data relating to [^{3}H]fucose and [^{3}H]cholesterol transport were obtained primarily in connection with previous studies, although the results presented here were not reported in those publications (24, 25). In short, transported [^{3}H]fucosylated glycoprotein was determined as contralaterally corrected acid-insoluble radioactivity in optic pathway structures following intraocular injection of [5,6-^{3}H]fucose. Transported [^{3}H]cholesterol was determined as contralaterally corrected radioactivity in cholesterol (purified by thin-layer chromatography) following intraocular injection of [^{3}H]acetate.

RESULTS

Incorporation and Metabolism of Label at Injection Site

Total phospholipid, DPG, and protein in the retina were all rapidly labeled after injection of precursors, with maximal labeling of each reached by 1 h postinjection. The decay of these labeled components in the retina is shown in Fig. 1*A*. From 1 to 60 d the total phospholipid radioactivity declined with an apparent half-life of 7 d. DPG, which initially comprised 1–2% of the total lipid label, showed little if any loss of radioactivity until 24 d, after which it decayed with a half-life of 8 d. The decay of radioactivity in retinal proteins was multiphasic and was arbitrarily resolved into two components corresponding to apparent half-lives of 7 and 22 d during the ranges of 1–32 and 32–60 d, respectively.

Initially Transported Material

During the first few hours after injection, transported labeled protein, phospholipid, and DPG arrived and accumulated in the optic tracts and superior colliculi as shown in Fig. 2. Labeled protein arrived first in each structure, followed by total phospholipid, and then DPG. However, the time difference between the early accumulation in the optic tract and that

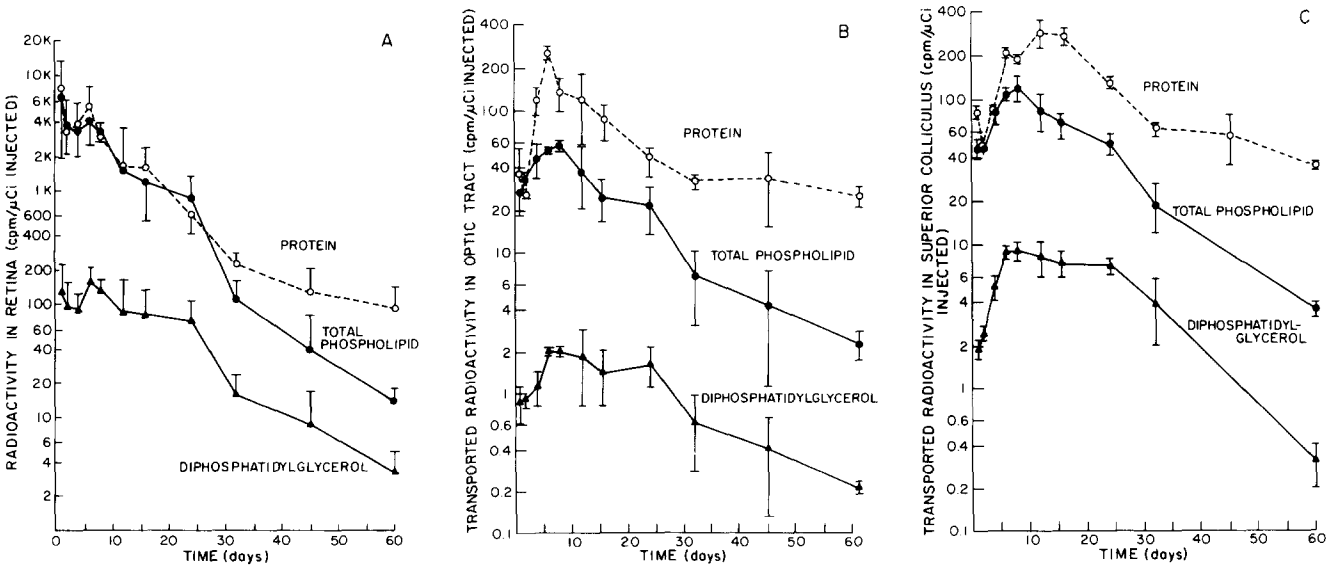

FIGURE 1 Long-term accumulation and turnover of labeled macromolecules in (*A*) retina, (*B*) optic tract, and (*C*) superior colliculus. Rats were injected intraocularly with [^{35}S]methionine and [2-^{3}H]glycerol, and 1–60 d later radioactivity was determined in protein (TCA-precipitable ^{35}S), total phospholipid (lipid-soluble ^{3}H), and DPG (^{3}H in the purified lipid). In each case, radioactivity in the appropriate contralateral structure was subtracted. Each value represents the mean ±SD of three to six animals.

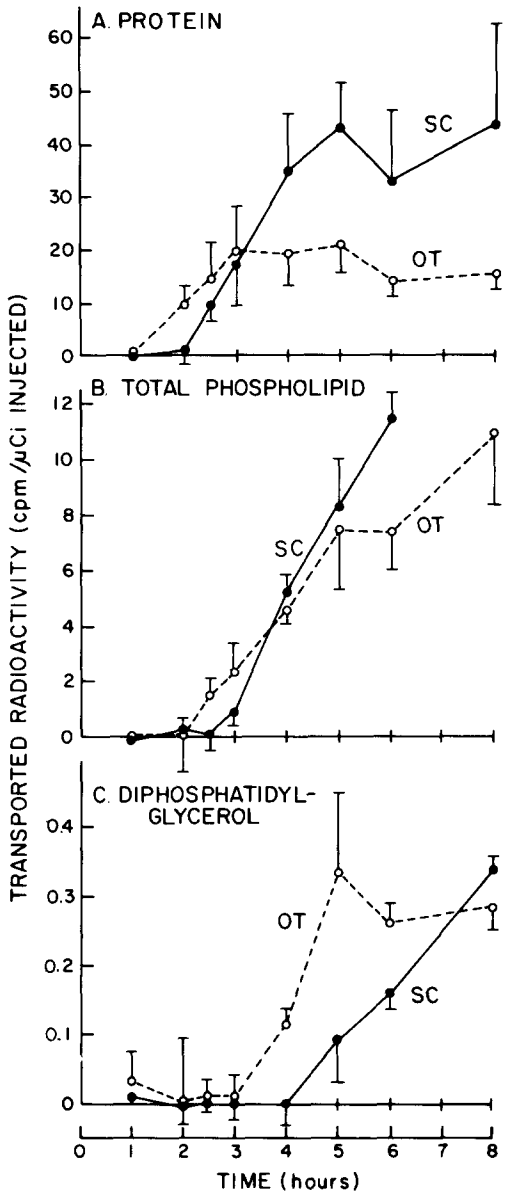

FIGURE 2 Time-course of arrival and accumulation of transported labeled macromolecules in the optic tract (*OT*, - - -) and superior colliculus (*SC*, ——). Rats were injected intraocularly with [^{35}S]methionine and [2-^{3}H]glycerol, and 1–8 h later contralaterally corrected radioactivity was determined in protein (*A*), total phospholipid (*B*), and DPG (*C*). Each value represents the mean ±SD of three to four animals.

in the superior colliculus was approximately the same for protein and total phospholipid (~40 min), whereas that for DPG was longer (~75 min). This time difference is a more accurate indicator of transport rate than the arrival time because it is independent of synthesis and processing lags in the retina. Based on an optic tract-to-superior colliculus distance of 9.5–10.5 mm, rates of 300–400 mm/d for protein and total phospholipid and 180–200 mm/d for DPG were calculated. These rates and a retina-to-superior colliculus distance of 18–20 mm indicate that retinal processing times were ~1 h for protein and 1.5 h for total phospholipid and DPG. This correction for retinal processing time perhaps accounts for the somewhat faster rapid transport rate calculated here relative to the rates obtained in previous studies of the mammalian optic system (12, 25–27).

Accumulation and Metabolism of Transported Material

The long-term accumulation and turnover of these transported components in the optic tract and superior colliculus are shown in Fig. 1 *B* and *C*. Total phospholipid and DPG peaked at ~1 wk in both structures. The accumulation of protein was more complex, showing a wave of slow transport which peaked at 6 and 12 d in the optic tract and superior colliculus, respectively. For each component, the patterns of the loss of radioactivity through 60 d were similar in the retina, optic tract, and superior colliculus. Transported protein showed a biphasic decay, whereas, most of the transported total phospholipid decayed with a half-life of ~10 d. In all the visual structures, there was little loss of radioactivity from DPG for several weeks, after which it decayed in a manner very similar to that of total phospholipid.

In double-label experiments, the ^{32}P:^{3}H ratio of total phospholipid and DPG was followed from 4 to 32 d (Fig. 3). Although this ratio in total phospholipid tended to increase, especially from 4 to 15 d, the DPG ratio was essentially constant.

In control experiments involving colchicine, the drug treatment at the level used usually blocked the transport of total phospholipid and DPG by >90% at 8 h and 1 d after isotope injection (three of five experiments). In some animals, the blockage was not complete (20–70% inhibition), probably due to injection variability, because the 1-μg pretreatment dose used is at a sharp inflection in the dose-response curve (28). In such cases, transported total phospholipid and DPG were decreased in parallel in the visual pathway structures of any one animal. Incorporation of radioactivity into retinal macromolecules was unaffected by the drug treatment.

The relative distribution of various transported components among visual system structures at times after precursor injection is shown in Fig. 4. Fucose-labeled glycoproteins, which peaked in the superior colliculus at 8 h (25), showed a strong preference for accumulation at nerve endings (lateral geniculate and superior colliculus) at all times after 6 h. Methionine-labeled proteins showed a larger accumulation in nerve endings than in axons (optic nerve and optic tract) from 4 h to 1 d. At 2 d, the optic nerve showed a high level of labeled protein, probably due to the entry of slowly transported proteins from the retina, and by 12 d the peak of radioactivity again resided in the nerve endings. In contrast, transported cholesterol was preferentially deposited in the optic nerve at all times studied,

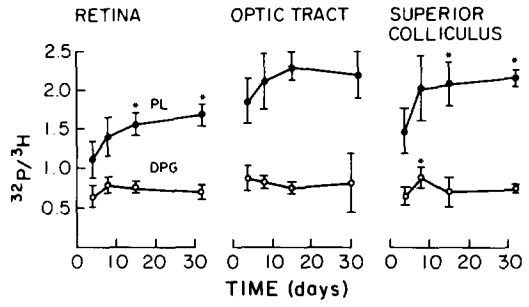

FIGURE 3 ^{32}P:^{3}H ratio of contralaterally corrected labeled total phospholipid (*PL*, ●) and DPG (○) in visual structures. Rats were injected intraocularly with 60 μCi of [^{32}P]orthophosphate and 200 μCi of [2-^{3}H]glycerol and killed 4–32 d later. Each value represents the mean ± SD of three animals. Asterisks (*) indicate significant differences from 4-d values ($p < 0.05$).

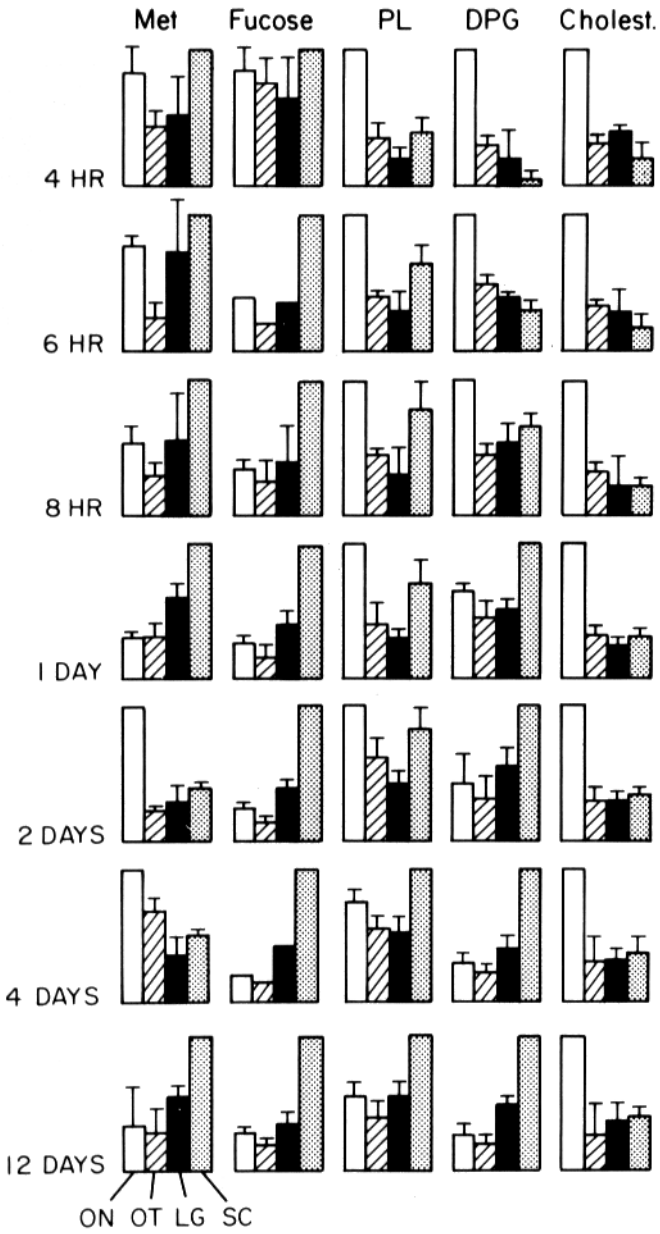

FIGURE 4 Relative distribution of labeled transported macromolecules among optic pathway structures at various times after intraocular injection of precursors. *ON*, optic nerve; *OT*, optic tract; *LG*, lateral geniculate; *SC*, superior colliculus. Optic nerve and tract segments are of approximately equal length. Values in each histogram are normalized to the highest value which is set as full scale. *Met*, [^{35}S]methionine-labeled, TCA-precipitable material (protein); *Fucose*, [^{3}H]fucose-labeled, TCA-precipitable material (glycoprotein); *PL*, [2-^{3}H]glycerol-labeled, lipid-soluble material (phospholipid); *DPG*, [2-^{3}H]glycerol-labeled DPG; *Cholest.*, [^{3}H]acetate-labeled cholesterol. Values are expressed as the mean ± SD of three to six animals, except those for fucose at 6 h and 4 d, which are from single experiments.

even though it was rapidly transported and continued to accumulate in all optic pathway structures for at least 30 d (24). The time-course of the phospholipid distribution was intermediate between the two extremes shown by fucose and cholesterol. A distribution showing comparable labeling of axons and nerve endings was established in 6–8 h and maintained for about 2 d. During the next few days the labeling pattern changed such that by ~6 d the nerve endings were preferentially labeled and the label in the optic nerve and tract equalized (optic nerve and tract are approximately the same length). The DPG distribution showed a gradual shift toward the nerve endings so that by 2–4 d the distribution resembled that of fucose.

Enrichment of DPG in Mitochondria

1 wk after intraocular injection of [^{32}P]orthophosphate, a mitochondrial fraction was prepared from pooled superior colliculi. Portions of the homogenate and of the mitochondrial fraction were subjected to thin-layer chromatography, and DPG radioactivity, as a percentage of total phospholipid radioactivity, was determined. The homogenate contained 2% of phospholipid radioactivity as DPG. Although the yield of radioactive mitochondria in the pellet was low (accounting for 3.5% of the total radioactivity), it was sixfold enriched in this lipid, 12% of the [^{32}P]radioactivity being present as DPG.

DISCUSSION

DPG Metabolism

There is a considerable body of evidence that DPG, and the enzymes specific for its synthesis, are confined exclusively to the inner mitochondrial membrane (18, 19, 29). The other major lipids found in mitochondria are synthesized in the endoplasmic reticulum and then exchanged with mitochondrial lipids via soluble exchange proteins (19, 30, 31). Most of the evidence in support of these statements has been obtained in experiments using liver or heart mitochondria. However, available subcellular fractionation data in brain systems indicate that in the brain, also, DPG is a mitochondrial-specific marker (32, 33). Careful studies of phospholipid composition of other purified brain subcellular membrane fractions such as microsomes (32, 34), myelin (35), synaptic plasma membrane (36), and synaptic vesicles (37) demonstrate the absence of significant quantities of DPG. Our own data concerning subcellular distribution of [^{32}P]phosphate-labeled DPG also support this consensus. Our values, 2 and 12%, respectively, for [^{32}P]DPG content as a percentage of total radioactive phospholipids in homogenate and mitochondra, correlate quite well with the observed concentrations of this lipid as a percentage of total phospholipid, which has been reported as 2.2% in brain (38) and 14.1% for brain mitochondria (39). This relative enrichment is also compatible with the estimate that ~15% of brain protein can be accounted for by mitochondria (33).

The possibility that the observed DPG metabolism represented, in part, appearance of DPG in glial cells (either from *de novo* synthesis of degraded axonal phospholipid or by direct transfer of DPG from axonal structures to glial structures) was considered unlikely. Although autoradiographic evidence (40) demonstrated that radioactivity from axonal phospholipids can be transferred to myelin, this process is vastly more efficient with reusable phospholipid precursors such as choline than with the nonreusable precursor [2-^{3}H]glycerol. In a relevant biochemical study, Haley and Ledeen (41) come to a similar conclusion with respect to transfer to myelin of radioactivity from [2-^{3}H]glycerol or [^{14}C]serine in axonally transported lipids in optic tract. With respect to cytoplasmic structures, transfer of radioactivity of [2-^{3}H]glycerol-labeled lipids from the preganglionic axons of the ciliary ganglion to "Schwann cell cytoplasm remained at an exceedingly low level" (40). It is also relevant to note that, at least in liver, label in microsomal lipids that are transferred to mitochondria is not reincorporated into

DPG (42). All this suggests that labeled DPG in visual structures is a true marker for transport of mitochondria in retinal ganglion cells.

The turnover of total phospholipid is initially more rapid than that of DPG, which is relatively stable for 2–3 wk in all parts of the optic pathway. That this is true even in the retina suggests that metabolic stability of DPG is intrinsic to mitochondria and not related to the kinetics of mitochondrial or total phospholipid transport and accumulation. Qualitatively similar results have been reported for liver mitochondria. Radioactivity in DPG was not lost until several days after an intraperitoneal injection of [^{32}P]phosphate, even though turnover in other mitochondrial and microsomal lipids begins within hours (42). These decay kinetics may be related to a life cycle involving turnover of whole mitochondria. We suggest that much of the DPG label is incorporated during a period of net synthesis of mitochondrial components related to binary fission. The DPG is then metabolically stable until these "new" mitochondria begin to be engulfed and degraded ~3 wk later. This initial period of metabolic stability renders less likely the alternate possibility that label is incorporated into DPG by a random replacement of preexisting molecules during metabolic turnover. That the ^{32}P:^{3}H ratio of DPG is nearly constant from 4 to 32 d also supports the idea of its initial metabolic stability. In contrast, the trend toward an increasing ^{32}P:^{3}H ratio for total phospholipid suggests that once a lipid is degraded the ^{32}P is reusable more efficiently than is the rapidly metabolized [^{3}H]glycerol (43). However, the ratio changes are not great for any phospholipid because released ^{32}P, localized in visual structures, is enchanging against a large pool of nonradioactive phosphate in the brain.

Model for Dynamics of Mitochondrial Transport

We have interpreted our data in terms of a model (Fig. 5) in which individual axonal mitochondria move randomly by way of occasional, rapid, saltatory motions with no directional bias, and in which there is a constant exchange of mitochondria among the nerve cell pools (cell body, axon, and nerve endings). This model is based in part on optical studies of axons (1, 3–6). Most relevant is the work of Forman et al. (3) who reported that individual rod-shaped particles (presumably mitochondria), although usually stationary, occasionally undergo saltatory translocations. According to our model, statistically, a small proportion of the labeled mitochondria would make predominantly orthograde movements with few stops and could travel from the cell body to the nerve endings with a rate approaching that of the saltatory motions (the 200-mm/d rate measured here). However, most of the radioactive mitochondria become displaced along the axon more slowly due to frequent stops and direction reversals. With time, the labeled mitochondria become equilibrated throughout the cell and the relative distribution of label among the various parts of the optic pathway ceases to change. We find that the distribution pattern of transported labeled DPG in the visual structures actually changes little after 2 d, even though the accumulation of label does not peak in these structures until about 7 d. This would indicate that there are two processes involved in the equilibration of mitochondria within the neuron. First, newly labeled mitochondria in the cell body slowly equilibrate with those in the axon, accounting for the 1-wk period required for maximum accumulation in the nerve and tract. Second, labeled mitochondria in the axons rapidly equilibrate with the nerve ending pool on a time scale that is probably shorter (~1 d)

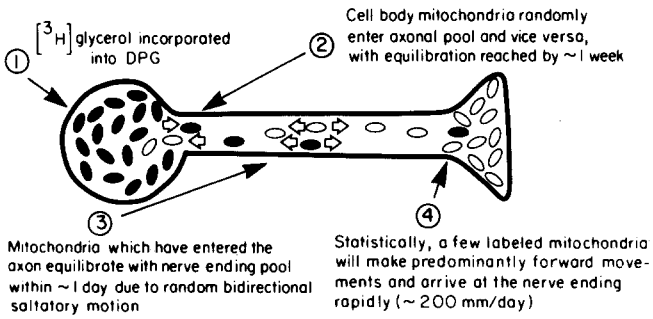

FIGURE 5 Model for the dynamics of mitochondrial movement in the neuron. Dark and light mitochondria represent labeled and unlabeled mitochondria, respectively.

than the 2–4 d indicated in Fig. 4 (the distribution is constantly being perturbed by feed-in of label from the cell body). The sections of optic nerve and optic tract that we dissect are similar in length, suggesting that the rough equivalence in DPG radioactivity at equilibrium corresponds to an equal distribution of mitochondria in both structures. Also, at equilibrium, distribution of labeled DPG reveals that the number of mitochondria in the nerve endings (lateral geniculate plus superior colliculus) is about three times that in the axon (optic nerve plus optic tract). A possible explanation for the greater number might be related to a large volume of nerve endings (this might be severalfold greater than that of axons in optic tract and optic nerve if there is enough branching). Thus, the larger amount of radioactive DPG in superior colliculus and lateral geniculate body might reflect a greater volume of neuronal processes that contain mitochondria at the same concentration as in axons. Alternatively, there may actually be a concentration of mitochondria at nerve endings as a result either of mitochondria leaving the transport mechanism entirely for long periods of time or of a change in affinity for the transport mechanism which results in a lower average residence time for mitochondria on the transport mechanism. Quantitative ultrastructural studies might resolve this issue. The large number of cell types within the retina (most of which do not project out of the retina) precludes a similar estimation of the relative size of the ganglion cell body pool.

This model is compatible with previous studies in which transported proteins were labeled with amino acid precursors and the accumulation of radioactivity in nerve-ending mitochondria monitored by subcellular fractionation (7–9, 12) or electron microscopic autoradiography (10, 13, 44). Although accumulation of radioactive mitochondria was seen to be a protracted process, some nerve-ending mitochondria were labeled rapidly. More recently, Lorenz and Willard (45) calculated a transport rate for labeled mitochondrial F_1-ATPase in the rabbit visual system of about one-quarter their fast transport rate.

There are two lines of evidence that are not consistent with this model. First, data concerning the transport of protein-bound ^{59}Fe (in mitochondrial cytochromes) through the chicken sciatic nerve were interpreted as indicating a very slow transport rate (11). However, this methodology is complicated by the prolonged incorporation of the ^{59}Fe into mitochondrial cytochromes, which results in a continued increase in the specific activity of the mitochondria entering the sciatic nerve during much of the time period studied. This may result in a large underestimate of the transport rate. Second, in nerve ligation studies, mitochondria or mitochondrial markers have been found to slowly accumulate equally on both sides of a

ligature (14–17). In our model, ligation should not result in accumulation because individual mitochondria move bidirectionally and there is no concerted movement of mitochondria. We suggest that a ligation may result in local damage to the transport mechanism so that some mitochondria that move into the ligation area are stranded there, resulting in artifactual accumulation.

The mechanism of the bidirectional saltatory motion and its relationship to the motion of other transported material are not addressed by our experiments. However, our model is consistent with some aspects of the general model proposed by Ochs (46) in which transported materials attach with different affinities to a bidirectional mobile carrier.

Distribution of Transported Molecules

We have identified several distribution patterns of transported labeled material among axons and terminals (Fig. 4), which we explain as follows. (*a*) Some molecules may be uniquely destined for specific cell membrane regions. Fucose-labeled glycoproteins may be in this category because they are preferentially deposited into the nerve-ending structures. (*b*) As transported membranous particles travel through the axon, certain of their constituent molecules may rapidly exchange with equivalent molecules in structural membranes. The distribution of transported cholesterol can be explained by this mechanism in that the small pool of labeled cholesterol in particles committed to fast transport may rapidly exchange with a large, unlabeled pool in the axonal structural membranes. By the time the transported particles reach the optic tract, much of the labeled cholesterol has been replaced with unlabeled cholesterol from the large pool in nonmotile structures. This exchange process may also involve much of the phospholipid, because initially a distribution is established in which the optic nerve is more highly labeled than the optic tract. However, a significant amount of labeled phospholipid reaches the nerve ending, indicating that the exchange process is not so extensive as with cholesterol. Eventually, the transported molecules initially deposited in one region of the neuron may be redistributed to other regions. For example, phospholipid label in the optic nerve is higher than in the optic tract for the first 2 d, but by 6 d they have equalized. A similar redistribution phenomenon for protein has been reported in peripheral nerve (47). Interpretation of the bulk phospholipid data is, of course, complicated by the fact that this is a heterogeneous class of molecules which is represented in all membranous structures. (*c*) A molecule may be localized exclusively within an independent organelle. This is the case for DPG, which is localized entirely within mitochondria, which in turn distribute according to pool size independent of other cell structures.

This research was supported in part by U. S. Public Health Service grants NS-11615, ND-16371, and HD-03110.

Received for publication 18 November 1980, and in revised form 29 January 1981.

REFERENCES

1. Breuer, A. C., C. N. Christian, M. Henkart, and P. G. Nelson. 1975. Computer analysis of organelle translocation in primary neuronal cultures and continuous cell lines. *J. Cell Biol.* 65:562–576.
2. Cooper, P. D., and R. S. Smith. 1974. The movement of optically detectable organelles in myelinated axons of *Xenopus laevis*. *J. Physiol. (Lond.).* 242:77–97.
3. Forman, D. S., A. L. Padjen, and G. R. Siggins. 1977. Axonal transport of organelles visualized by light microscopy: cinemicrographic and computer analysis. *Brain Res.* 136: 197–213.
4. Kirkpatrick, J. B., J. J. Bray, and S. M. Palmer. 1972. Visualization of axoplasmic flow *in vitro* by Normarski microscopy. Comparisons to rapid flow of radioactive proteins. *Brain Res.* 43:1–10.
5. Leestma, J. G., and S. S. Freeman. 1977. Computer-assisted analysis of particulate axoplasmic flow in organized CNS tissue cultures. *J. Neurobiol.* 8:453–467.
6. Smith, R. S. 1972. Detection of organelles in myelinated nerve fibers by dark-field microscopy. *Can. J. Physiol. Pharmacol.* 50:467–469.
7. Cancalon, P. 1979. Subcellular and polypeptide distributions of slowly transported proteins in the garfish olfactory nerve. *Brain Res.* 161:115–130.
8. Cancalon, P., and L. M. Beidler. 1975. Distribution along the axon and into various subcellular fractions of molecules labelled with [^{3}H]leucine and rapidly transported in the garfish olfactory nerve. *Brain Res.* 89:225–244.
9. Cuénod, M., and J. Schonbach. 1971. Synaptic proteins and axonal flow in the pigeon visual pathway. *J. Neurochem.* 18:809–816.
10. Droz, B., H. L. Koenig and L. DiGiamberardino. 1973. Axonal migration of protein and glycoprotein to nerve endings. I. Radioautographic analysis of the renewal of protein in nerve endings of chicken ciliary ganglion after intracerebral injection of [^{3}H]lysine. *Brain Res.* 60:93–127.
11. Jeffrey, P. L., K. A. C. James, A. D. Kidman, A. M. Richards, and L. Austin. 1972. The flow of mitochondria in chicken sciatic nerve. *J. Neurobiol.* 3:199–208.
12. Karlsson, J.-O., and J. Sjöstrand. 1971. Synthesis, migration and turnover of protein in retinal ganglion cells. *J. Neurochem.* 18:749–767.
13. Schonbach, J., Ch. Schonbach, and M. Cuénod. 1973. Distribution of transported proteins in the slow phase of axoplasmic flow. An electron microscopical autoradiographic study. *J. Comp. Neurol.* 152:1–16.
14. Zelená, J. 1968. Bidirectional movements of mitochondria along axons of an isolated nerve segment. *Z. Zellforsch. Mikrosk. Anat.* 92:186–196.
15. Banks, P., D. Mangnall, and D. Mayor. 1969. The redistribution of cytochrome oxidase, noradrenaline and adenosine triphosphate in adrenergic nerves constricted at two points. *J. Physiol. (Lond.).* 200:745–762.
16. Khan, M. A., and S. Ochs. 1975. Slow axoplasmic transport of mitochondria (MAO) and lactic dehydrogenase in mammalian nerve fibers. *Brain Res.* 96:267–277.
17. Partlow, L. M., C. D. Ross, R. Motwani, and D. B. McDougal, Jr. 1972. Transport of axonal enzymes in surviving segments of frog sciatic nerve. *J. Gen. Physiol.* 60:388–405.
18. Davidson, J. B., and N. Z. Stanacev. 1971. Biosynthesis of cardiolipin in mitochondria. *Can. J. Biochem.* 49:1117–1124.
19. Hostetler, K. Y., and H. Van Den Bosch. 1972. Subcellular and submitochondrial localization of the biosynthesis of cardiolipin and related phospholipids in rat liver. *Biochim. Biophys. Acta.* 260:380–386.
20. Skipski, V. P., and M. Barclay. 1969. Thin layer chromatography of lipids. *Methods Enzymol.* 14:530–598.
21. Wiggins, R. C., S. L. Miller, J. A. Benjamins, J. A. Krigman, and P. Morell. 1976. Myelin synthesis during postnatal nutritional deprivation and subsequent rehabilitation. *Brain Res.* 107:257–273.
22. Horrocks, L. A., and G. Y. Sun. 1972. Ethanolamine plasmalogens. *In* Research Methods in Neurochemistry, Vol. 31A, L. Fleischer and L. Packer, editors. Academic Press, Inc., New York. 223–232.
23. Tamir, H., M. M. Rapport, and L. Roisin. 1974. Preparation of synaptosomes and vesicles with sodium diatrizoate. *J. Neurochem.* 23:943–949.
24. Blaker, W. D., A. D. Toews, and P. Morell. 1979. Cholesterol is a component of the rapid phase of axonal transport. *J. Neurobiol.* 11:243–250.
25. Goodrum, J. F., A. D. Toews, and P. Morell. 1979. Axonal transport and metabolism of [^{3}H]fucose- and [^{35}S]sulfate-labeled macromolecules in the rat visual system. *Brain Res.* 176:255–272.
26. Schlicter, D. J., and W. O. McClure. 1974. Dynamics of axoplasmic transport in the optic system of the rat. *Exp. Brain Res.* 21:83–95.
27. Willard, M., W. M. Cowan, and P. R. Vagelos. 1974. The polypeptide composition of intra-axonally transported proteins: evidence for four transport velocities. *Proc. Natl. Acad. Sci. U. S. A.* 71:2182–2187.
28. Paulson, J. C., and W. O. McClure. 1974. Microtubules and axoplasmic transport. *Brain Res.* 73:333–337.
29. Stoffel, W., and H. Schiefer. 1968. Biosynthesis and composition of phosphatides in outer and inner mitochondrial membranes. *Hoppe-Seyler's Z. Physiol. Chem.* 349:1017–1026.
30. Miller, E. K., and R. M. C. Dawson. 1972. Can mitochondria and synaptosomes of guinea-pig brain synthesize phospholipds? *Biochem. J.* 126:805–821.
31. Miller, E. K., and R. M. C. Dawson. 1972. Exchange of phospholipids between brain membranes *in vitro*. *Biochem. J.* 126:823–835.
32. Eichberg, J., J. Whittaker, and R. M. C. Dawson. 1964. Distribution of lipids in subcellular particles of guinea-pig brain. *Biochem. J.* 92:91–100.
33. Abood, L. G. 1969. Brain mitochondria. *In* Handbook of Neurochemistry. A. Lajtha, editor. Plenum Press, New York. 2:303–326.
34. Tamai, Y., S. M. Araki, K. Katsuta, and M. Satake. 1974. Molecular composition of the submicrosomal membrane lipid of rat brain. *J. Cell Biol.* 63:749–758.
35. Norton, W. T. 1976. Formation, structure and biochemistry of myelin. *In* Basic Neurochemistry. G. J. Siegel, R. W. Albers, R. Katzman, and B. W. Agranoff, editors. Little, Brown & Co., Boston. 74–102.
36. Breckenridge, W. C., G. Gombos, and I. G. Morgan. 1972. The lipid compostion of adult rat brain synaptosomal plasma membrane. *Biochim. Biophys. Acta.* 266:695–707.
37. Breckenridge, W. C., I. G. Morgan, J. P. Zanetta, and G. Vincendon. 1973. Adult brain synaptic vesicles. II. Lipid composition. *Biochim. Biophys. Acta.* 320:681–686.
38. Wuthier, R. E. 1968. Two-dimensional chromatography on silica gel-loaded paper for the microanalysis of polar lipids. *J. Lipid Res.* 7:544–550.
39. Getz, G. S., W. Bartley, D. Lurie, and B. M. Notton. 1968. The phospholipids of various sheep organs, rat liver, and of their subcellular fractions. *Biochem. Biophys. Acta.* 152:325–339.
40. Droz, B., M. Brunetti, L. DeGiamberardino, H. L. Koenig, and G. Porcellati. 1979. Transfer of phospholipid constituents to glia during axonal transport. *Soc. Neurosci. Symp.* 4:344–360.
41. Haley, J. E., and R. W. Ledeen. 1979. Incorporation of axonally transported substances into myelin lipids. *J. Neurochem.* 32:735–742.
42. McMurray, W. C., and R. M. C. Dawson. 1969. Phospholipid exchange reactions within the liver cell. *Biochem. J.* 112:91–108.
43. Miller, S. L., J. A. Benjamins, and P. Morell. 1977. Metabolism of glycerophospholipids of myelin and microsomes in rat brain. *J. Biol. Chem.* 252:4025–4037.
44. Schonbach, J., C. Schonbach, and M. Cuénod. 1971. Rapid phase of axoplasmic flow and synaptic proteins: an electron microscopical autoradiographic study. *J. Comp. Neurol.* 141: 485–498.
45. Lorenz, T., and M. Willard. 1978. Subcellular fractionation of intraaxonally transported polypeptides in the rabbit visual system. *Proc. Natl. Acad. Sci. U. S. A.* 75:505–509.
46. Ochs, S. 1974. Systems of material transport in nerve fibers (axoplasmic transport) related to nerve function and trophic control. *Ann. N. Y. Acad. Sci.* 228:202–223.
47. Ochs, S. 1975. Retention and redistribution of proteins in mammalian nerve fivers by axoplasmic transport. *J. Physiol. (Lond.).* 253:459–475.